BJP British Journal of Pharmacology

DOI:10.1111/bph.12119
www.brjpharmacol.org

RESEARCH PAPER

Pharmacological fractionation of tetrodotoxin-sensitive sodium currents in rat dorsal root ganglion neurons by μ-conotoxins

Min-Min Zhang[1], Michael J Wilson[1], Joanna Gajewiak[1], Jean E Rivier[3], Grzegorz Bulaj[2], Baldomero M Olivera[1] and Doju Yoshikami[1]

[1]*Department of Biology, University of Utah, Salt Lake City, UT, USA,* [2]*Department of Medicinal Chemistry, University of Utah, Salt Lake City, UT, USA, and* [3]*The Clayton Foundation Laboratories for Peptide Biology, The Salk Institute, La Jolla, CA, USA*

Correspondence
Doju Yoshikami, Department of Biology, University of Utah, 257 South 1400 East, Salt Lake City, UT 84112, USA. E-mail: yoshikami@bioscience.utah.edu

Keywords
μ-conotoxin PIIIA; μ-conotoxin SmIIIA; μ-conotoxin TIIIA; dorsal root ganglion; superior cervical ganglion; tetrodotoxin; voltage-gated sodium channel; whole-cell patch clamp

Received
29 August 2012
Revised
18 December 2012
Accepted
27 December 2012

BACKGROUND AND PURPOSE

Adult rat dorsal root ganglion (DRG) neurons normally express transcripts for five isoforms of the α-subunit of voltage-gated sodium channels: $Na_V1.1$, 1.6, 1.7, 1.8 and 1.9. Tetrodotoxin (TTX) readily blocks all but $Na_V1.8$ and 1.9, and pharmacological agents that discriminate among the TTX-sensitive Na_V1-isoforms are scarce. Recently, we used the activity profile of a panel of μ-conotoxins in blocking cloned rodent Na_V1-isoforms expressed in *Xenopus laevis* oocytes to conclude that action potentials of A- and C-fibres in rat sciatic nerve were, respectively, mediated primarily by $Na_V1.6$ and $Na_V1.7$.

EXPERIMENTAL APPROACH

We used three μ-conotoxins, μ-TIIIA, μ-PIIIA and μ-SmIIIA, applied individually and in combinations, to pharmacologically differentiate the TTX-sensitive I_{Na} of voltage-clamped neurons acutely dissociated from adult rat DRG. We examined only small and large neurons whose respective I_{Na} were >50% and >80% TTX-sensitive.

KEY RESULTS

In both small and large neurons, the ability of the toxins to block TTX-sensitive I_{Na} was μ-TIIIA < μ-PIIIA < μ-SmIIIA, with the latter blocking ≳90%. Comparison of the toxin-susceptibility profiles of the neuronal I_{Na} with recently acquired profiles of rat Na_V1-isoforms, co-expressed with various $Na_V\beta$-subunits in *X. laevis* oocytes, were consistent: $Na_V1.1$, 1.6 and 1.7 could account for all of the TTX-sensitive I_{Na}, with $Na_V1.1 < Na_V1.6 < Na_V1.7$ for small neurons and $Na_V1.7 < Na_V1.1 < Na_V1.6$ for large neurons.

CONCLUSIONS AND IMPLICATIONS

Combinations of μ-conotoxins can be used to determine the probable Na_V1-isoforms underlying the I_{Na} in DRG neurons. Preliminary experiments with sympathetic neurons suggest that this approach is extendable to other neurons.

Abbreviations

CAP, compound action potential; DRG, dorsal root ganglion; I_{Na}, sodium current; μ-PIIIA, μ-conotoxin PIIIA from *Conus purpurascens*; μ-SmIIIA, μ-conotoxin SmIIIA from *Conus stercusmuscarum*; μ-TIIIA, μ-conotoxin TIIIA from *Conus tulipa*; Na_V1, α-subunit of voltage-gated sodium channel; $Na_V\beta$, β-subunit of voltage-gated sodium channel; SCG, superior cervical ganglion; TTX, tetrodotoxin; VGSC, voltage-gated sodium channel

Introduction

Voltage-gated sodium channels (VGSCs) mediate action potentials in excitable tissues. VGSCs comprise a main, pore- and voltage sensor-bearing α-subunit, which alone can form a functional channel, and one or more accessory β-subunits, which modulate the expression and function of the α-subunit (Catterall *et al.*, 2007). There are nine isoforms of α-subunits, $Na_V1.1$ through to $Na_V1.9$, encoded in the mammalian genome (Goldin *et al.*, 2000). Two, $Na_V1.4$ and 1.5, are largely expressed in skeletal and cardiac muscle, respectively, and the remaining seven are largely expressed in neurons. With the exception of $Na_V1.8$ and 1.9, which are found almost exclusively in primary somatosensory neurons, all neuronal Na_V1-isoforms are very sensitive to tetrodotoxin (TTX), the classic pore blocker of VGSCs (Catterall *et al.*, 2005). It is of interest to obtain additional ligands that target VGSCs for a least two reasons. (i) Ligands that discriminate among the Na_V1-isoforms can be used to characterize the functional roles of specific channel isoforms in a neuron or neuronal circuit, and (ii) VGSCs are potential targets for ligands that can be developed into therapeutic drugs to treat a variety of neurological disorders ranging from epilepsy to pain (Momin and Wood, 2008; Catterall, 2010; Dib-Hajj *et al.*, 2010).

Studies on mRNA-transcript abundance show that $Na_V1.1$, 1.6, 1.7, 1.8 and 1.9 are the major Na_V1-isoforms normally expressed in adult rat dorsal root ganglion (DRG) neurons (Black *et al.*, 1996; Rush *et al.*, 2007; Fukuoka *et al.*, 2008) while $Na_V1.3$ is expressed only during early development but can be induced in adults in various pain models (Waxman *et al.*, 1994; Dib-Hajj *et al.*, 1999; Black *et al.*, 2004). In broad terms, the relative transcript abundances in adult rat DRG are as follows: $Na_V1.1$ is expressed to a limited extent in large neurons, $Na_V1.6$ is expressed in all sizes of neurons, $Na_V1.7$ is highly expressed in small neurons but also expressed in some large neurons, $Na_V1.8$ is expressed in small and medium neurons, while $Na_V1.9$ is expressed exclusively in small neurons (Dib-Hajj *et al.*, 2010). Thus, a given DRG neuron can express more than one Na_V1-isoform, and channel expression can be dynamic. This raises the issue of identifying the functional contributions of the different Na_V1-isoforms in a given DRG neuron. In the present study, we used μ-conotoxins to examine this matter.

Cone snail venom contains at least four different families of peptidic toxins that target VGSCs. Three of these, δ-, ι-, μO-conotoxins act as gating modifiers (Terlau and Olivera, 2004; Fiedler *et al.*, 2008; Lewis *et al.*, 2012) whereas the fourth, the μ-conotoxins, act by blocking the pore of VGSCs, much like TTX but with greater Na_V1-isoform selectivity (Zhang *et al.*, 2007; 2009; 2010). Recently, we characterized the ability of a panel of 11 μ-conotoxins to block cloned $Na_V1.1$ through to 1.8 (all from rat except $Na_V1.6$, which was from mouse) expressed in *Xenopus laevis* oocytes. (None of the μ-conotoxins blocked $Na_V1.8$.) We then tested members of the panel for their ability to block A- and C-compound action potentials (A- and C-CAPs, respectively) in rat sciatic nerve (Wilson *et al.*, 2011). The blocking profile of the μ-conotoxins led us to conclude that the major Na_V1-isoforms responsible for propagating action potentials in A- and C-fibres are, respectively, $Na_V1.6$ and $Na_V1.7$. Also, a contributor to C-CAPs was either or both $Na_V1.8$ or 1.9, insofar as TTX (1–10 μM) did not obliterate C-CAPs, although it significantly attenuated their amplitudes and reduced their conduction velocities (Wilson *et al.*, 2011).

However, susceptibility of A- and C-CAPs to VGSC antagonists provides only an indirect and qualitative indication of the identities of the underlying channels. A- and C-CAPs are meditated by fast- and slow- conducting axons of neurons with, respectively, large and small cell somas in DRG (Harper and Lawson, 1985). In the present study, we voltage clamped the soma of large and small neurons of acutely dissociated rat DRG preparations and examined the effects of three μ-conotoxins, μ-TIIIA (Lewis *et al.*, 2007), μ-PIIIA (Shon *et al.*, 1998) and μ-SmIIIA (West *et al.*, 2002), which are a subset of the μ-conotoxin panel mentioned above, on the TTX-sensitive sodium current (I_{Na}) of these neurons. These μ-conotoxins were selected because they were collectively best able, at a saturating or near-saturating concentration of 10 μM, to discriminate among rat $Na_V1.1$, 1.2, 1.6 and 1.7 exogenously expressed in *X. laevis* oocytes without or with Na_Vβ-subunit co-expression (Zhang *et al.*, 2012). To determine the probable molecular identities of the VGSCs underlying the I_{Na} in DRG neurons, we compared the μ-conotoxin-susceptibility profiles of I_{Na} in DRG neurons with those of channels expressed in oocytes.

We also examined the effects of these toxins on adult rat superior cervical ganglion (SCG) neurons; these sympathetic cells normally express transcripts for $Na_V1.3$, 1.6 and 1.7 (Rush *et al.*, 2006). The effects of the aforementioned three μ-conopeptides on $Na_V1.3$ expressed in *X. laevis* oocytes are known, but only in the absence of any Na_Vβ-subunit co-expression (Wilson *et al.*, 2011); however, by assuming that Na_Vβ-subunit co-expression does not markedly affect the affinity of the three μ-conotoxins for $Na_V1.3$, the experimental results could be reconciled with the Na_V1-isoform transcripts expressed by SCG neurons.

Methods

Dissociation of DRG and SCG neurons

Use of animals in this study followed protocols approved by the University of Utah's Institutional Animal Care and Use Committee that conform to the National Institutes of Health *Guide for the Care and Use of Laboratory Animals*. DRG and SCG neurons of adult Sprague Dawley rats of either sex were dissociated and used as described previously for DRG neurons (Zhang *et al.*, 2006). Briefly, rats were killed by exposure to CO_2 gas and ganglia were excised and treated with collagenase followed by trypsin. Cells were mechanically dissociated by trituration, washed and suspended in L15 medium supplemented with 14 mM glucose, 1 mM $CaCl_2$ and 10% FBS supplemented with penicillin/streptomycin. Dissociated DRG and SCG neurons were kept in suspension at 4°C for up to 3 days (Blair and Bean, 2002). All studies involving animals are reported in accordance with ARRIVE guidelines for reporting experiments involving animals (Kilkenny *et al.*, 2010; McGrath *et al.*, 2010).

Whole-cell patch-clamp recordings

Voltage-clamp recordings were performed with a MultiClamp 700A amplifier (Axon Instruments, Union City, CA,

USA) at room temperature in a bath with a total volume of 100 µL, essentially as previously described (Zhang *et al.*, 2006). The extracellular solution contained 140 mM NaCl, 3 mM KCl, 1 mM $MgCl_2$, 1 mM $CaCl_2$, 0.1 mM $CdCl_2$, 20 mM HEPES, pH 7.3. Recording pipettes had resistances of <2 MΩ and contained 140 mM CsF, 10 mM NaCl, 1 mM EGTA, 10 HEPES, pH 7.3; and series resistance compensation was >80%. After achieving whole-cell clamp conditions, recordings were not initiated until the holding current had settled, which required >10 min; the contribution of $Na_V1.9$, relative to that of $Na_V1.8$, to the TTX- resistant current of DRG neurons is minimized by such a settling period (Choi *et al.*, 2006). The membrane potential was held at –80 mV, and VGSCs channels were activated by a 50 ms test pulse to 0 mV, applied every 20 s. Current signals were low-pass filtered at 3 kHz, digitized at a sampling frequency of 10 kHz, and leak-subtracted by a P/6 protocol using in-house software written in LabVIEW (National Instruments, Austin, Texas, USA). The 0-mV test pulse was chosen because the activation *I-V* curves of TTX-sensitive I_{Na} and TTX-resistant I_{Na} peaked near –5 mV and 0 mV, respectively (not illustrated), close to values reported by others (Elliott and Elliott, 1993). Furthermore, when TTX-resistant point mutants of mouse $Na_V1.6$ and human $Na_V1.7$ were expressed in DRG neurons of $Na_V1.8$-null mice, which allowed the channels to be identified by their resistance to TTX, the TTX-resistant sodium currents peaked near 0 and –10 mV respectively (Herzog *et al.*, 2003). The peaks of the *I-V* curves for all of the aforementioned currents varied by ≤5% over a 10-mV span; thus, we used a 0-mV test pulse as a convenient compromise that we presumed would activate all of the Na_V1-isoforms in DRG neurons essentially to the same extent. SCG neurons displayed *I-V* curves that peaked at 0 mV (not illustrated); thus, the 0-mV test pulse protocol described above was also used for SCG neurons, which have only TTX-sensitive sodium currents whose *I-V* curve peaks at 0 mV (Liu *et al.*, 2012).

Toxins and their application

µ-Conotoxins were synthesized as previously described [(Wilson *et al.*, 2011) and references therein]. TTX was obtained from Alomone Labs (Jerusalem, Israel). All toxins were dissolved in extracellular solution and applied to the neurons studied by simple bath exchange by manually applying, with a pipette, toxin solution (150 µL) at one end of the boat-shaped chamber (volume, 100 µL) while simultaneously withdrawing solution at the other end of the chamber over a time span of <20 s. (The patch electrode was used to lift the cell from the underlying substrate and position the cell near the upstream part of the chamber to ensure that the cell was fully exposed to the introduced toxin solution.) Toxin exposures were conducted in a static bath to conserve toxin, while washout of toxin was done by continuous perfusion with extracellular solution (at a rate of 0.6 mL·min^{-1}), essentially as in previous experiments (Zhang *et al.*, 2006; 2007). Although the method of toxin application precluded accurate measurement of the rate of onset of block, the continuous and relatively rapid (4-bath volumes·min^{-1}) perfusion during toxin washout is expected to provide a reliable assessment of the reversibility of the toxins.

The level of TTX-resistant I_{Na} of each DRG cell was determined by perfusion with 1 µM TTX following tests with µ-conotoxins [none of which blocked TTX-resistant I_{Na} (Wilson *et al.*, 2011)].

Estimation of the relative contributions of $Na_V1.1$, 1.6 and 1.7 to the overall TTX-sensitive I_{Na} of individual DRG neurons from the levels of block produced by µ-TIIIA, µ-PIIIA and µ-SmIIIA

We recently examined µ-TIIIA, µ-PIIIA and µ-SmIIIA on rat $Na_V1.1$, 1.6 and 1.7 expressed in *X. laevis* oocytes with and without co-expression with $Na_V\beta$-subunits (Zhang *et al.*, 2012). From the reported K_d or IC_{50} values, the expected levels of block at a toxin concentration of 10 µM were calculated (see Table 2). The co-expression of $Na_V\beta$-subunits affected the percentage block, with co-expression of either β1 or β3 increasing it and co-expression of either β2 or β4 decreasing it, but in no case was the change greater than 10%. To simplify the calculations below, we used the percentage block values of Na_V1-isoforms obtained without any $Na_V\beta$-subunit co-expression (see Table 2) and values <5% were set to zero. Three types of sequential toxin-application protocols were used: application of µ-TIIIA followed by µ-PIIIA (Type 1 test), or µ-PIIIA followed by µ-SmIIIA (Type 2 test), or µ-TIIIA followed by µ-PIIIA then by µ-SmIIIA (Type 3 test), and the contributions of $Na_V1.1$, 1.6 and 1.7 to the TTX-sensitive I_{Na} were estimated, as described below.

The abbreviations '$fe_{1.1}T$', '$fe_{1.6}T$' and '$fe_{1.7}T$' are the fractional efficacies of µ-TIIIA in blocking $Na_V1.1$, 1.6 and 1.7, respectively. The same abbreviations but with the suffixes 'P' or 'Sm' (replacing 'T') are the corresponding fe values for µ-PIIIA and µ-SmIIIA respectively. Values of fe are as follows (cf. Table 2): for µ-TIIIA, $fe_{1.1}T = 0.92$, $fe_{1.6}T < 0.05 \approx 0.0$ and $fe_{1.7}T < 0.02 \approx 0.0$; for µ-PIIIA, $fe_{1.1}P = 0.99$, $fe_{1.6}P = 0.99$ and $fe_{1.7}P < 0.02 \approx 0.0$; and for µ-SmIIIA, $fe_{1.1}Sm = 1.00$, $fe_{1.6}Sm = 0.99$ and $fe_{1.7}Sm = 0.97$.

The percentage of I_{Na} blocked by each of µ-TIIIA, µ-PIIIA and µ-SmIIIA is represented by %T, %P and %Sm respectively. The fraction of overall current blocked by a given µ-conotoxin is the linear sum of the percentage of each Na_V1-isoform present multiplied by the fractional efficacy of that µ-conotoxin in blocking that isoform, that is:

$$\%T = \%Na_V1.1 * fe_{1.1}T,$$

$$\%P = \%Na_V1.1 * fe_{1.1}P + \%Na_V1.6 * fe_{1.6}P, \text{ and}$$

$$\%Sm = \%Na_V1.1 * fe_{1.1}Sm + \%Na_V1.6 * fe_{1.6}Sm + \%Na_V1.7 * fe_{1.7}Sm.$$

(The third, or last, equation is listed for formality and not used.) Given these equations, $\%Na_V1.1$, $\%Na_V1.6$ and $\%Na_V1.7$ were determined as follows.

Rearranging the first equation yields,

$$\%Na_V1.1 = \%T / fe_{1.1}T = \%T * 1.08 \quad (1)$$

Rearranging the second equation yields,

$$\%Na_V1.6 = (\%P - (\%Na_V1.1 * fe_{1.1}P)) / fe_{1.6}P.$$

Substituting $\%Na_V1.1$ of Eqn. 1 and noting that the block of $Na_V1.1$ by μ-TIIIA is readily reversible (Zhang *et al.*, 2012) yields,

$$\%Na_V1.6 = (\%P\ (\%T/fe_{1.1}T)*fe_{1.1}P)/fe_{1.6}P = \%P*0.99 - \%T*1.09. \quad (2)$$

Since $\%Na_V1.1 + \%Na_V1.6 + \%Na_V1.7 = 100\%$,

$$\%Na_V1.7 = 100\% - \%Na_V1.6 - \%Na_V1.1.$$

Substituting $\%Na_V1.1$ and $\%Na_V1.6$ from Eqns. 1 and 2,

$$\%Na_V1.7 = 100\% - \%T*1.08 - \%P*0.99 + \%T*1.09,$$

or simplifying

$$\%Na_V1.7 = 100\% - \%P*0.99 + \%T*0.01. \quad (3)$$

When μ-TIIIA was not used (i.e. Type 2 tests), since $fe_{1.1}P = fe_{1.6}P = 0.99$,

$$\%Na_V1.7 = 100\% - \%P/0.99. \quad (4)$$

Thus, the values of $\%Na_V1.1$, $\%Na_V1.6$ and $\%Na_V1.7$ were obtained from Eqns. 1, 2 and 3, respectively, in Type 1 and Type 3 tests. Values of $\%Na_V1.7$ were obtained in Type 2 tests from Eqn. 4.

(It might be noted that since the coefficients of the variables in Eqns. 1 through 4 are very close to either 1.0 or 0.0, the percentages of the different Na_V1-isoforms can be simply approximated as follows: $\%Na_V1.1 \approx \%T$, $\%Na_V1.6 \approx \%P - \%T$ and $\%Na_V1.7 \approx 100\% - \%P$.)

Because of the relative slowness of the block of the I_{Na} of DRG neurons by (10 μM) μ-SmIIIA, steady-state block was not always achieved before the cell was lost or other tests initiated. In such cases, the time course of block was fit to a single-exponential function and the calculated plateau was used as an estimate of steady-state block.

Estimation of the relative contribution of $Na_V1.3$ to the overall I_{Na} of individual SCG neurons from the levels of block produced by μ-TIIIA, μ-PIIIA and μ-SmIIIA

These three μ-conotoxins have been tested on $Na_V1.3$ expressed in *X. laevis* oocytes *without* co-expression of any $Na_V\beta$-subunits, where it was observed that the K_d for the block by μ-SmIIIA was 0.035 ± 0.014 μM and IC_{50}s for the block by μ-PIIIA and μ-TIIIA were 3.2 ± 0.81 and 7.9 ± 1.9 μM respectively (Wilson *et al.*, 2011). If it is assumed that co-expression with $Na_V\beta$-subunits does not affect the block by these toxins, then it can be calculated (by use of these K_d and IC_{50} values together with the equation in footnote of Table 2) that VGSCs with $Na_V1.3$ as the α-subunit will be blocked by 100, 76 and 56% upon exposure to 10 μM μ-SmIIIA, μ-PIIIA and μ-TIIIA respectively. These percentage block values were used in the Discussion to calculate the fraction of I_{Na} in SCG neurons attributable to $Na_V1.3$.

Data analysis

Curve fittings were done with homemade software written in LabVIEW (National Instruments). Averaged data are expressed as means with minimum and maximum observed (or calculated) values.

Results

In general, large DRG neurons have mostly TTX-sensitive I_{Na} whereas small neurons have mostly TTX-resistant I_{Na}. To more accurately measure TTX-sensitive I_{Na} of small neurons, we chose to use only small DRG neurons in which the majority of I_{Na} was TTX-sensitive – this was facilitated by visually selecting the smallest of the small DRG neurons. In total, we examined the I_{Na} of 32 small and 41 large DRG neurons by whole-cell voltage clamping as described in Methods, and the results from all of these cells are presented in Supporting Information Table S1. Cell size was quantified by electrical capacitance (Figure 1A and Supporting Information Table S1). If the cells are assumed to be spherical with a specific membrane capacitance of 1 $\mu F \cdot cm^{-2}$ (Hille, 2001), the calculated average diameter was 20 μm (range, 13–24 μm) for small cells and 40 μm (range, 33–54 μm) for large cells. These values are consistent with the diameters visually estimated with an eyepiece micrometer; the large cells appeared more or less spherical, while most of the small cells had an ellipsoidal appearance. A total of 21 SCG neurons were examined, and results from these cells are presented in Supporting Information Table S2; these sympathetic neurons were largely spherical, with some having stubby bumps, presumably vestigial dendrites.

TTX-sensitivities of large versus small DRG neurons

The percentage of I_{Na} blocked by 1 μM TTX for small cells ranged from 55 to 100% (average, 79%) and that for large cells ranged from 80 to 100% (average, 96%); the distribution of TTX-sensitivities as a function of cell size, as measured by membrane capacitance, is shown in Figure 1A. Sample recordings of I_{Na} from each of the two size classes in the absence and presence of TTX are shown in Figure 1B.

Sensitivities of large versus small DRG neurons to μ-conotoxins μ-TIIIA, μ-PIIIA and μ-SmIIIA, each applied individually to separate cells

The sodium currents of voltage-clamped neurons were challenged by μ-TIIIA, μ-PIIIA or μ-SmIIIA, with each μ-conotoxin applied at a concentration of 10 μM, as described in Methods (Figure 2). Of the small neurons, eight were tested with μ-TIIIA (which produced an average block of 6%, range 0–12%), seven with μ-PIIIA (which produced an average block of 27%, range 11–45%) and two with μ-SmIIIA (which produced an average block of 98%, range 98–99%). Of the large neurons, seven were tested with μ-TIIIA (which produced an average block of 30%, range 12–48%), eight with μ-PIIIA (which produced an average block of 78%, range 60–90%) and three with μ-SmIIIA (which produced an average block of 95%, range 94–96%). Thus, for TTX-sensitive I_{Na} of both small and large neurons, the order of level of block produced was μ-TIIIA < μ-PIIIA < μ-SmIIIA.

Figure 2A shows that the block by μ-TIIIA for both sized cells was readily reversible; this reversibility was observed in

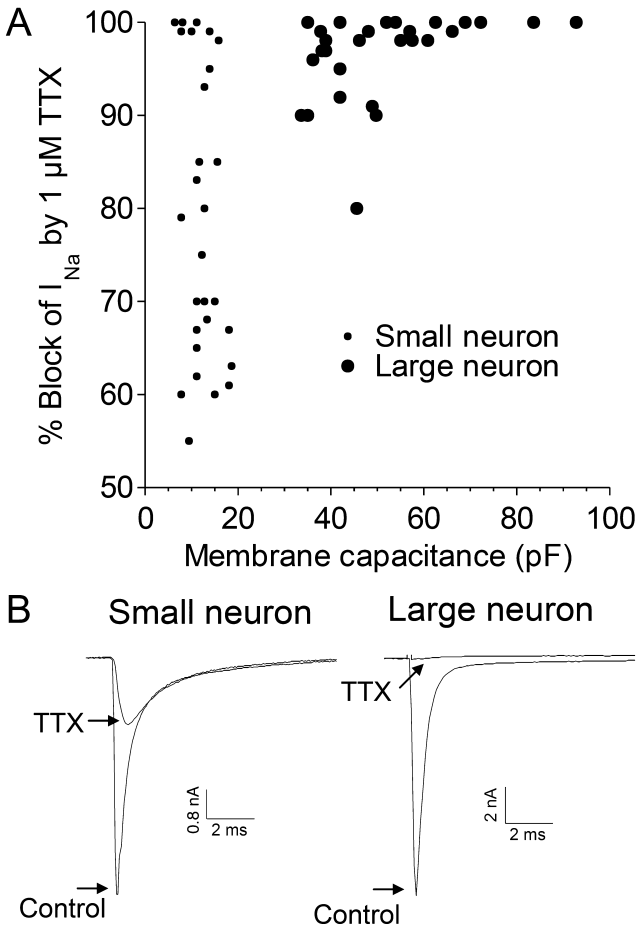

Figure 1

TTX-sensitivities of I_{Na} and membrane capacitances of small versus large DRG neurons. Acutely dissociated DRG neurons were whole-cell patch clamped as described in Methods, and I_{Na} was obtained by stepping the potential to 0 mV from a holding potential of –80 mV. Responses in the presence of TTX (1 μM) are those when steady-state block was achieved. (A) Percentages of peak I_{Na} blocked by TTX as a function of membrane capacitance, a reflection of cell size. Small neurons, identified as such by visual inspection under the microscope, had lower membrane capacitances than large neurons (note their mutually exclusive distributions) and broader range of TTX-sensitivities than large neurons. (B) Examples of current traces obtained in the absence and presence of 1 μM TTX. Note, the TTX-resistant I_{Na} inactivates more slowly than the TTX-sensitive I_{Na}. Traces are from small cell 505a and large cell 309A/L1 in Supporting Information Table S1. In subsequent figures, the TTX-resistant peak I_{Na} was subtracted from total peak I_{Na} to obtain the 'TTX-sensitive I_{Na}.'

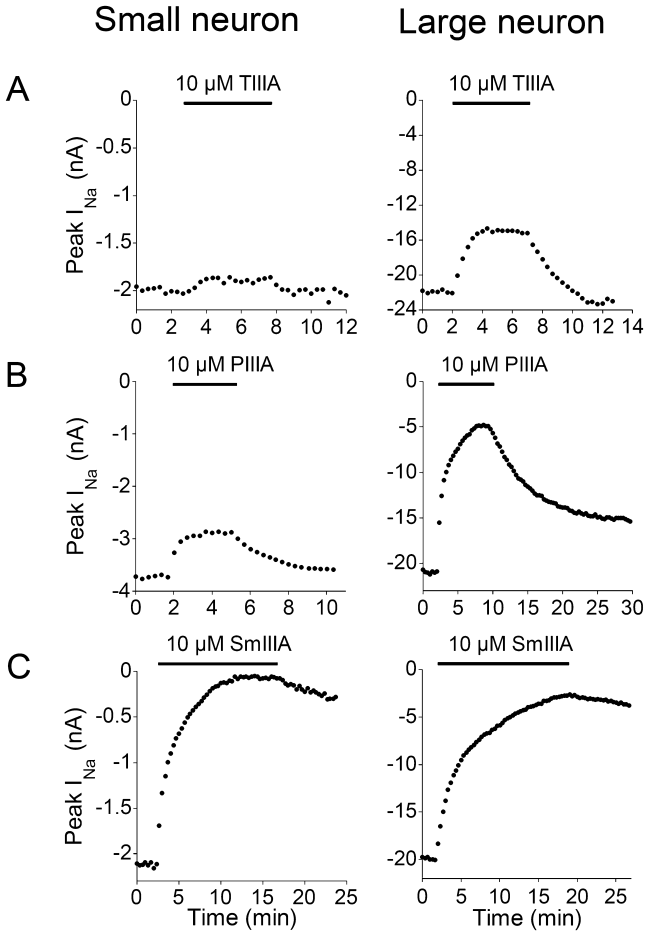

Figure 2

Time course of block of TTX-sensitive I_{Na} of small versus large neuron by μ-TIIIA, μ-PIIIA or μ-SmIIIA, each tested individually at a concentration of 10 μM. Recordings of I_{Na} were obtained as in Figure 1. The plots are peaks of TTX-sensitive I_{Na} obtained every 20 s before, during and after exposure to the indicated μ-conotoxin, denoted by bar at top of each plot. Each plot is an example from a different cell. (A) Block by μ-TIIIA was much less for small than large neuron, and this block was rapidly reversible for both sizes. (B) Similarly, block by μ-PIIIA was greater for large than small neuron. (C) Nearly complete block of TTX-sensitive I_{Na} was achieved with μ-SmIIIA for both small and large neurons. Data are from small neurons 504b, 621c and 621f and large neurons 622A, 504B and 428A in Supporting Information Table S1.

all the cells tested. The recovery from block followed single-exponential time courses with average τ_{off} values of 0.7 ± 0.12 min (mean ± SEM, n = 4) for small cells and 1.1 ± 0.2 min (n = 5) for large cells. Thus, the block by μ-TIIIA was invariably rapidly reversible.

To be able to make more quantitative comparisons of the functional expression of the Na_V1-isoforms, trials of a given cell to successive exposures to different μ-conotoxins were performed, as described below.

Sensitivities of large versus small DRG neurons to successive applications of μ-TIIIA, μ-PIIIA or μ-SmIIIA

The I_{Na} of voltage-clamped DRG neurons were also challenged by serial applications of at least two μ-conotoxins. Three sorts of serial-exposure tests were employed as detailed in Methods. An example of a trial with sequential application of all three μ-conotoxins (i.e. a Type 3 test) is presented in Figure 3. The results from Type 3, as well as those from Type 1 and Type 2 tests, are summarized in Figure 4. The general observations here are consistent with results from exposures to individual toxins described above. The I_{Na} of small neurons

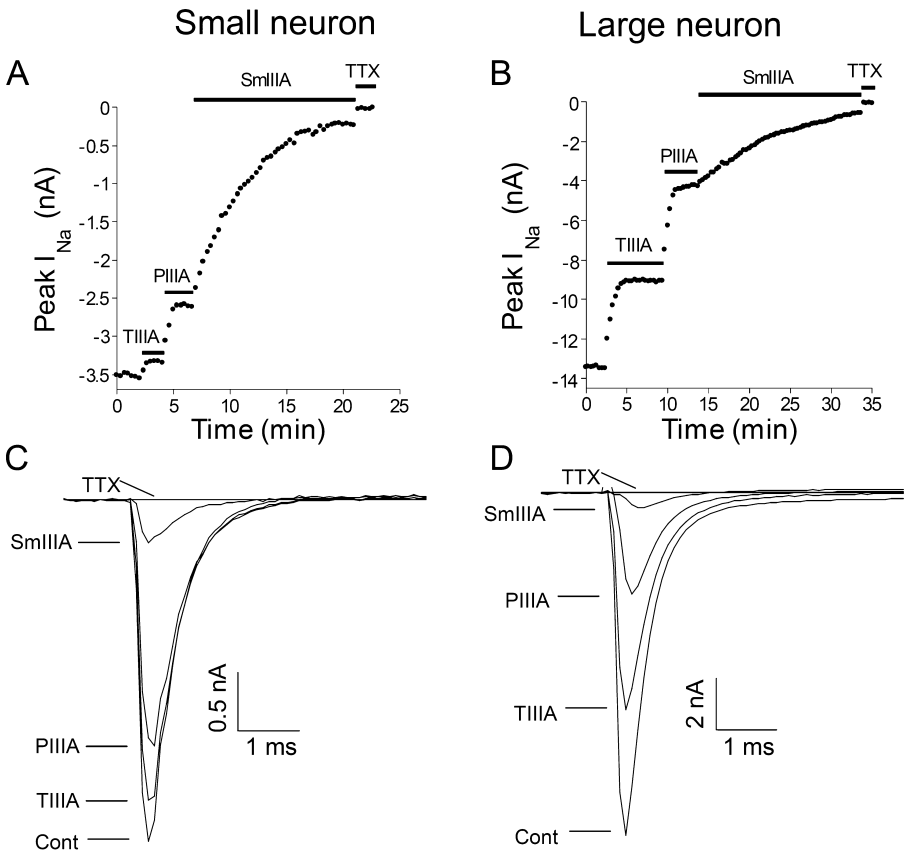

Figure 3

Cumulative block of TTX-sensitive I_{Na} of small versus large DRG neuron during sequential applications of μ-TIIIA, μ-PIIIA and μ-SmIIIA. Recordings of I_{Na} were obtained as in Figure 2 except the three toxins were successively applied to a given neuron (Type 3 test). (A and B) Examples of time courses of block of TTX-sensitive I_{Na} from small (A) and large (B) neurons; horizontal bar represents time during which the indicated μ-conotoxin was present. Note, block by TTX (1 μM) is 100%, reflecting that only the TTX-sensitive I_{Na} is presented in these plots. (C and D) Examples of I_{Na} traces obtained during each of the four steady-state phases in panel A (control, and during exposure to each of μ-TIIIA, μ-PIIIA and μ-SmIIIA). Data are from cells 614b/S4 and 309A/L1 in Supporting Information Table S1.

were minimally (7%) blocked by μ-TIIIA, somewhat more by μ- PIIIA (23%) and largely (94%) blocked by μ- SmIIIA; on the other hand, the I_{Na} of large neurons was blocked significantly by μ-TIIIA (30%) and μ-PIIIA (71%), with additional block provided by μ-SmIIIA (96%) (Figure 4A). As will be explained in the Discussion, we attribute the I_{Na} blocked by TIIIA to be due to $Na_V1.1$, the additional I_{Na} block by PIIIA to be due to $Na_V1.6$ and the remaining I_{Na} (which is blocked by SmIIIA) to be due to $Na_V1.7$ (see Figure 6).

The distribution of the block by μ-TIIIA and μ-PIIIA of I_{Na} of individual cells are illustrated in Figure 4B. μ-TIIIA had no effect on the I_{Na} of some small cells but blocked the I_{Na} of all large cells at least to some degree. Remarkably, for two large cells, μ-TIIIA blocked 70% of the I_{Na}. μ-PIIIA had an effect on all small and large cells, with a greater effect on large, than on small, cells – so much so that the distributions did not overlap.

Sensitivity of SCG neurons to μ-TIIIA, μ-PIIIA and μ-SmIIIA applied individually or sequentially

A total of 21 sympathetic neurons were examined in experiments that paralleled those involving DRG neurons described above. When applied individually, the rank order of block of the peak I_{Na} of SCG neurons by 10 μM of each toxin was (average % block, range of % block): μ-TIIIA (11.0%, 5%–25%) < μ-PIIIA (31.0%, 22%–45%) < μ-SmIIIA (95.8%, 94%–97%), where μ-TIIIA, μ-PIIIA and μ-SmIIIA were tested on 12, 4 and 5 neurons respectively (see Supporting Information Table S2). Just as with DRG neurons, the block of SCG neurons by μ-TIIIA and μ-PIIIA was readily reversible whereas the block by SmIIIA was only slowly reversible – sample time courses of block and washout are illustrated in Supporting Information Figure S1.

SCG neurons were also tested by successive exposures to μ-TIIIA first, then μ-PIIIA, followed by μ-SmIIIA (each at 10 μM). An example of the resulting time course of block is shown in Figure 5A, and the current traces acquired during steady-state block with each toxin are shown in Figure 5B. The block of peak I_{Na} in these cases were (average % block, range of % block): μ-TIIIA (12.1%, 6%–25%), μ-PIIIA (33.6%, 11%–46%) and μ-SmIIIA (96.3%, 95%–99%), for eight neurons (see Supporting Information Table S2 for raw data). These % block values were close to the respective values without prior exposure to any μ-conotoxin (see preceding paragraph), and the results from SCG neurons exposed indi-

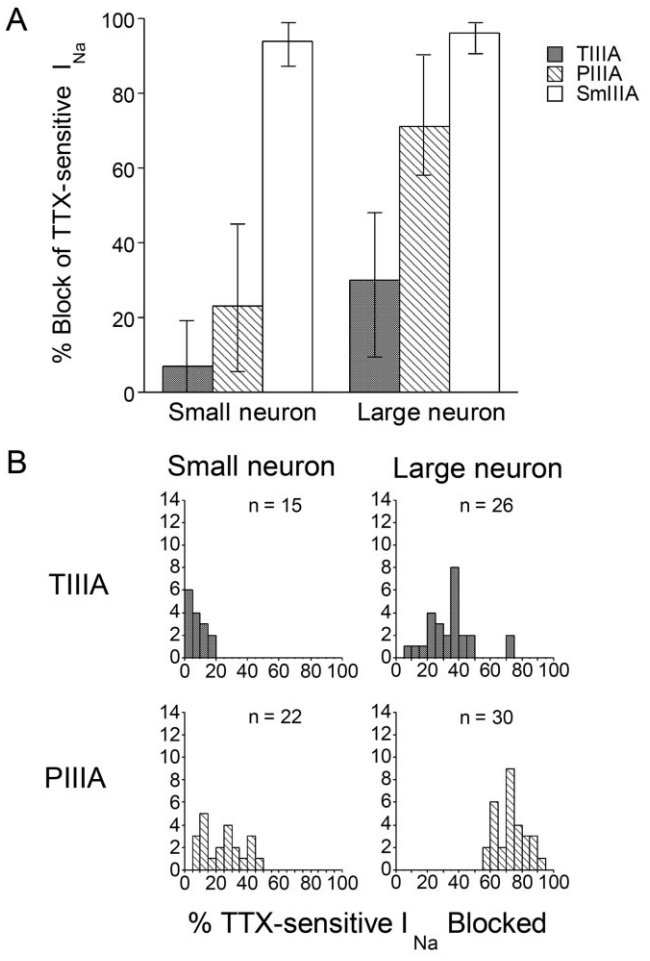

Figure 4

Pharmacological analysis of TTX-sensitive I_{Na} of large compared to small DRG neurons by μ-TIIIA, μ-PIIIA or μ-SmIIIA. Recordings of I_{Na} were obtained as in Figures 2 and 3. (A) Average percentage block of TTX-sensitive I_{Na} by μ-TIIIA, μ-PIIIA or μ-SmIIIA. 'Error bars' associated with each μ-conotoxin denote the minimum and maximum % block values, which are also evident in (B). (Cell numbers, or *n*-values, were as follows: μ-TIIIA, 15 small and 24 large neurons; μ-PIIIA, 22 small and 30 large neurons; μ-SmIIIA, 16 small and 18 large neurons). (B) Distributions of cells with TTX-sensitive I_{Na} blocked by μ-TIIIA or μ-PIIIA in (A). μ-TIIIA had little or no effect on six of the small cells (≤5% block of I_{Na}). All large cells had some μ-TIIIA-susceptible I_{Na}, with two outliers (not included in panel A), which had an I_{Na} that was blocked by 70%. All large and small cells had μ-PIIIA-susceptible I_{Na}, but with mutually exclusive distributions of percentage I_{Na} blocked. Data are from cells listed in Supporting Information Table S1.

vidually or sequentially to the three μ-conotoxins were combined and are illustrated in Figure 5C (see also Supporting Information Table S2).

Discussion and conclusions

TTX-resistant I_{Na} in small versus large DRG neurons

It has long been known that in rat DRG, small neurons express TTX-resistant I_{Na} at a higher level than do large neurons and that the TTX-resistant I_{Na} inactivates more slowly than TTX-sensitive I_{Na} (Caffrey *et al.*, 1992; Ogata and Tatebayashi, 1992; Roy and Narahashi, 1992). Our results (Figure 1) are consistent with these reports. To be able to more accurately measure the block of TTX-sensitive I_{Na} in these experiments, we tested only small neurons in which most (i.e. >50%) of the total I_{Na} was TTX-sensitive – on visual inspection these turned out to be among the very smallest neurons.

Identification of the Na_V1-isoforms corresponding to the I_{Na} of DRG neurons that are blocked by μ-TIIIA, μ-PIIIA and μ-SmIIIA

The μ-conotoxins pharmacologically differentiated the TTX-sensitive I_{Na} of rat DRG neurons into three fractions. To translate the pharmacological profiles of the I_{Na} into the molecular species of VGSCs, we employed our recently acquired μ-conotoxin-susceptibility profiles of rat Na_V1-isoforms co-expressed with $Na_V\beta$-subunits in *X. laevis* oocytes (Zhang *et al.*, 2012). Table 2 shows the expected block of $Na_V1.1$, 1.6 and 1.7, expressed in oocytes, by the three μ-conotoxins at a concentration of 10 μM. This concentration is sufficiently removed from the K_d and IC_{50} values (regardless of $Na_V\beta$-subunit co-expression) that an *almost* all-or-none block is expected of each toxin-channel combination. Equations 1 through to 4 in Methods take into account the *almost* factor to provide more accurate estimates of the percentages of the channels involved.

Thus, the information in Table 2 was used to translate the results in Table 1 to produce Table 3, which shows the predicted levels of $Na_V1.1$, 1.6, 1.7 and 1.8 in several small and large neurons. Likewise, the data in Figure 4A was translated to produce Figure 6, which shows the average percentage contributions of $Na_V1.1$, 1.6 and 1.7 to the TTX-sensitive I_{Na} from many small and large neurons.

The results, taken as whole, provide the following overall picture: $Na_V1.1$, 1.6 and 1.7 are functionally expressed by all large and most small neurons. $Na_V1.7$ predominates in small neurons, but the levels of all three Na_V1-isoforms are rather similar in large neurons. The results from individual cells show that the relative levels of a given Na_V1-isoform can vary over a large range. This is particularly evident in small cells for $Na_V1.1$ and $Na_V1.8$, where two of five cells expressed no detectable levels of $Na_V1.1$ (i.e. μ-TIIIA produced no block) and the levels of $Na_V1.8$ ranged from essentially 0 to 37% (Tables 1 and 3). It is well known (e.g. Elliott and Elliott, 1993) that the relative contribution of TTX-resistant channels of small cells can vary over a wide range just as we found (Figure 1A); in view of this precedent, our observed variation in relative levels of the different TTX-sensitive Na_V1-isoforms is not unexpected.

Possible involvement of $Na_V1.2$ or 1.3 in DRG neurons

μ-TIIIA also potently blocks $Na_V1.2$ expressed in oocytes; however, the recovery from block of $Na_V1.2$ (τ_{off} = 37–100 min) was more than an order of magnitude slower than that of $Na_V1.1$ (τ_{off} = 1–2 min) (the range of τ_{off} values encompass the variation due to co-expression of $Na_V\beta1$-$\beta4$)

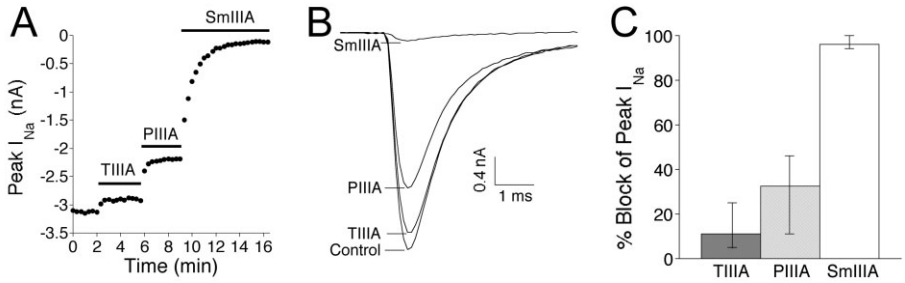

Figure 5

Susceptibility of I_{Na} of SCG neurons to μ-TIIIA, μ-PIIIA and μ-SmIIIA, each at 10 μM. Acutely dissociated SCG neurons were voltage-clamped as described in Methods. The experimental protocol used here essentially mimicked that of Figure 3 for DRG neurons. (A) Example of time course of block of I_{Na} of an SCG neuron during sequential application of the three μ-conotoxins; horizontal bars represent time during which indicated μ-conotoxins were present. (B) Example of I_{Na} traces obtained during each of the four steady-state phases in panel A (control, and during exposure to each of μ-TIIIA, μ-PIIIA and μ-SmIIIA). Data are from cell 1204a in Supporting Information Table S2. (C) Average percentage block of TTX-sensitive I_{Na} by μ-TIIIA, μ-PIIIA or μ-SmIIIA. 'Error bars' associated with each μ-conotoxin denote the minimum and maximum percentage block values. Cell numbers, or *n*-values, were as follows: μ-TIIIA, 12 neurons; μ-PIIIA, 12 neurons; μ-SmIIIA, 13 neurons. Data are from cells listed in Supporting Information Table S2.

Table 1

Pharmacological fractionation of the TTX-sensitive I_{Na} of five small and nine large neurons from rat DRG by successive exposures to 10 μM each of μ-TIIIA, μ-PIIIA and lastly μ-SmIIIA (Type 3 tests)

			% Block[d] of I_{Na} by		
Cell[a]	Capacitance[b] (pF)	TTX-s I_{Na}[c] (%)	μ-TIIIA	μ-PIIIA	μ-SmIIIA
S1	12.8	93	19	40	97
S2	15.7	85	0	10	93
S3	10	99	18	30	90
S4	18.6	63	13	28	95
S5	12.3	75	0	10	88
Ave.	13.88	83	10	24	93
L1	37.8	99	37	70	97
L2	83.7	100	17	58	95
L3	92.8	100	30	72	96
L4	57	99	23	70	94
L5	49.8	90	35	88	97
L6	66	99	45	85	95
L7	39	98	40	65	95
L8	57.5	98	38	77	99
L9	69	100	37	70	97
Ave.	61.4	98	34	73	96

[a]Prefix 'S' or 'L' indicates small or large neuron (cells corresponding to these are identified in Supporting Information Table S1).
[b]Electrical capacitance of cell.
[c]Percentage of total I_{Na} that was TTX-sensitive.
[d]Percentage of TTX-sensitive I_{Na} blocked by 10 μM of the indicated μ-conotoxin in Type 3 tests (see Methods).

(Zhang *et al.*, 2012). Thus, the uniformly rapid reversibility of the block of I_{Na} in DRG by μ-TIIIA (e.g. Figure 2A) is consistent with the block of $Na_V1.1$, but not that of $Na_V1.2$. By this

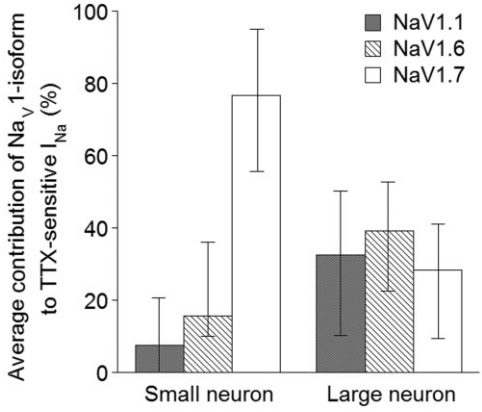

Figure 6

Breakdown of the contributions of $Na_V1.1$, 1.6, and 1.7 to the TTX-sensitive I_{Na} in rat DRG neurons. Percentages of TTX-sensitive I_{Na} of small and large DRG neurons contributed by $Na_V1.1$, 1.6 or 1.7 were calculated from μ-conotoxin-susceptibilities using Eqns. 1 through to 4 in Methods with information from Figure 4A and provided in Supporting Information Table S1. Expression levels of $Na_V1.1$ and 1.6 were calculated from data obtained from six small and 17 large neurons involving experiments where μ-TIIIA and μ-PIIIA were successively applied (Type 1 and 3 tests), while expression levels of $Na_V1.7$ were calculated from data obtained from 14 small and 13 large neurons involving experiments where μ-PIIIA and μ-SmIIIA were successively applied (Type 2 and 3 tests). Average percentage values are presented, with 'error bars' representing minimum and maximum observed values.

criterion, $Na_V1.2$ does not appear to be functionally expressed in any of the DRG neurons we examined.

$Na_V1.3$ was not considered in our assessment because, as noted in the Introduction, its transcript is not present in DRG of normal animals. A μ-conotoxin is not available yet that has sufficient specificity towards $Na_V1.3$ to evaluate its contribution in experiments such as those reported above.

Table 2

Percentage block based on oocyte data of I_{Na} of $Na_V1.1$, 1.6 or 1.7 with and without $Na_V\beta$-subunit co-expression, produced by 10 μM μ-SmIIA, μ-PIIIA or μ-TIIIA[a]

	μ-SmIIIA		μ-PIIIA		μ-TIIIA	
	K_d (μM)	% Block at 10 μM	K_d (μM)	% Block at 10 μM	K_d/IC_{50}[b] (μM)	% Block at 10 μM
$Na_V1.1$	0.0038	100	0.053	99	0.90[b]	92
+β1	0.0024	100	0.014	100	0.71[b]	93
+β2	0.07	99	0.14	99	1.7[b]	85
+β3	0.0023	100	0.017	100	0.48[b]	95
+β4	0.3	97	0.37	96	1.66[b]	86
$Na_V1.6$	0.069	99	0.081	99	>200	<5
+β1	0.046	100	0.005	100	>200	<5
+β2	0.75	93	0.243	98	>200	<5
+β3	0.059	99	0.009	100	>200	<5
+β4	0.403	96	0.951	91	>200	<5
$Na_V1.7$	0.26	97	570	<2	>570	<2
+β1	0.13	99	570	<2	>570	<2
+β2	1.5	87	570	<2	>570	<2
+β3	0.11	99	570	<2	>570	<2
+β4	1.17	90	570	<2	>570	<2
+β1+β2	0.38	96	570	<2	>570	<2
+β1+β4	0.55	95	570	<2	>570	<2
+β3+β2	0.2	98	570	<2	>570	<2
+β3+β4	0.35	97	570	<2	>570	<2

[a]K_d and IC_{50} values are oocyte data from Table 2 of (Zhang *et al.*, 2012).
[b]Value is K_d, but if it has a superscript 'b', value is IC_{50}. Percentage block was calculated with the equation % Block = 100%/(1 + C/10 μM), where C is K_d or IC_{50}.

Identification of the Na_V1-isoforms corresponding to the I_{Na} of SCG neurons that are blocked by μ-TIIIA, μ-PIIIA and μ-SmIIIA

A limitation of our approach is that the conversion of μ-conotoxin susceptibility into Na_V1-isoform identity depends critically on the assumption that the quantitative μ-conotoxin pharmacology of VGSCs exogenously expressed in *X. laevis* oocytes can be applied to endogenous channels in DRG neurons. This assumption remains to be validated. In an attempt to at least partially address this matter, we tested the three μ-conotoxins on SCG neurons, which express transcripts for $Na_V1.3$, 1.6 and 1.7 (Rush *et al.*, 2006). In other words, SCG neurons express $Na_V1.3$ unlike DRG neurons, which express $Na_V1.1$. Based on oocyte data, 10 μM μ-TIIIA is anticipated to block only 56% of $Na_V1.3$ (see penultimate paragraph in Methods) in comparison to ≥85% block of $Na_V1.1$ (Table 2). Use of μ-TIIIA at a concentration near its IC_{50} value for $Na_V1.3$ may be expected to yield more variable results than when used at saturating or near-saturating concentrations; however, at the latter concentrations μ-TIIIA would start to block $Na_V1.6$, and as a compromise we tested SCG neurons with 10 μM μ-TIIIA (the same concentrations as used on DRG neurons).

Exposure of SCG neurons to 10 μM μ-TIIIA alone blocked an average of 11% of the I_{Na} (n = 12 neurons (see Figure 5C and Supporting Information Table S2). Since 10 μM μ-TIIIA negligibly blocks $Na_V1.6$ and 1.7 expressed in oocytes (by <5%, Table 2), this suggests that 11%/0.56, or 19.6%, of the overall I_{Na} in SCG neurons involved $Na_V1.3$. (For the value of 0.56 in the divisor, see penultimate paragraph of Methods).

Exposure of SCG neurons to 10 μM μ-PIIIA blocked an average of 32.8% of the I_{Na} (n = 12 neurons, Figure 5C and Supporting Information Table S2). Assuming 19.6% of the overall I_{Na} is due to $Na_V1.3$ (see preceding paragraph), of which μ-PIIIA might be expected to block 76% (see penultimate paragraph of Methods), we surmise that 19%•0.76, or 14.4%, of the I_{Na} blocked by μ-PIIIA could be attributed to $Na_V1.3$. This leaves 32.8% minus 14.4%, or 18.4%, of the overall I_{Na} to be likely to be due to $Na_V1.6$, assuming $Na_V1.6$ to be largely blocked by μ-PIIIA (Table 2).

The remaining I_{Na}, 100% minus 18.4% (due to $Na_V1.6$) minus 19.6% (due to $Na_V1.3$), which equals 62%, was presumably due to $Na_V1.7$. Exposure to 10 μM μ-SmIIIA blocked an average of 96.1% of the I_{Na} (n = 13 neurons, Figure 5C and Supporting Information Table S2). This high, but incomplete,

Table 3

Predicted contributions of Na_V1-isoforms to TTX-sensitive I_{Na} (left) and total I_{Na} (right) of small and large DRG neurons

	TTX-sensitive I_{Na} % Contribution[b] by:			Total I_{Na} % Contribution[c] by:			
Cell[a]	$Na_V1.1$	$Na_V1.6$	$Na_V1.7$	$Na_V1.1$	$Na_V1.6$	$Na_V1.7$	$Na_V1.8$
S1	21	20	59	19	19	55	7
S2	0	10	90	0	9	76	15
S3	19	11	70	19	11	69	1
S4	14	14	72	9	9	45	37
S5	0	10	90	0	8	67	25
L1	40	31	29	39	31	29	1
L2	19	40	41	19	40	41	0
L3	33	40	27	33	40	27	0
L4	25	46	29	25	45	29	1
L5	38	51	11	34	46	10	10
L6	49	37	14	48	37	14	1
L7	44	22	34	43	22	33	2
L8	41	37	22	40	36	22	2
L9	40	31	29	40	31	29	0

[a]Numbering of small (S) and large (L) neurons of Table 1 is retained.
[b]Contribution of the indicated Na_V1-isoform to the TTX-sensitive I_{Na} of the cell, calculated from data in Tables 1 and 2 with Eqns. 1, 2, 3 & 4 in Methods.
[c]Percentage block data for each cell in the left half of this table were normalized to obtain the relative contributions of the Na_V1-isoforms to the total I_{Na} of each cell, with TTX-resistant I_{Na} attributed to the TTX-resistant isoform $Na_V1.8$ (Methods).

block by 10 μM SmIIIA is consistent with its behaviour in the oocyte expression system, where 10 μM μ-SmIIIA blocked $Na_V1.3$ by 100% (see penultimate paragraph of Methods), $Na_V1.6$ by 93 to 100% and $Na_V1.7$ by 87 to 99% (Table 2). Thus, we propose that the percentage contributions to the overall I_{Na} of SCG neurons are approximately as follows: 20% by $Na_V1.3$, 20% by $Na_V1.6$ and 60% by $Na_V1.7$. Essentially, the same percentage contributed by each Na_V1-isoform was found by confining the data to only the eight SCG neurons that had been sequentially exposed to μ-TIIIA, μ-PIIIA and μ-SmIIIA (Supporting Information Table S3).

Our overall conclusions regarding SCG neurons (albeit preliminary because we have yet to ascertain the effects of $Na_V\beta$-subunit co-expression on the activities of the μ-conotoxins against $Na_V1.3$) are consistent with our conclusions regarding DRG neurons.

It should be noted that the VGSC kinetics of SCG neurons were slower than that for both large and small DRG neurons (compare Figure 5B with Figure 3C and D). This difference in gating kinetics was also observed with neurons isolated from DRG and SCG from the same animal and tested essentially at the same time (not illustrated). $Na_V\beta$-subunits and other factors can affect channel gating (for recent reviews see Dib-Hajj and Waxman, 2010; Brackenbury and Isom, 2011; Chahine and O'Leary, 2011), and these might differ between SCG and DRG neurons, a possibility that awaits further examination.

Other limitations of the results

Another limitation of our results is that they inform us of the Na_V1-isoforms only in the plasma membrane of cell soma and not of axons and their termini. There is good electrophysiological evidence in primary sensory neurons for non-homogeneous distribution of TTX-resistant channels between soma and axon (Villière and McLachlan, 1996), and even between axon and its peripheral termini (Brock *et al.*, 1998; Strassman and Raymond, 1999).

A third limitation of our findings is that the reason(s) underlying the large variation in apparent relative expression levels of the various Na_V1-isoforms within a DRG cell-size class (Tables 1 and 3) have not been determined. It is possible that the observed heterogeneity is a consequence of the trauma the neurons experienced during dissociation. However, we suggest that the neurons may be inherently heterogeneous in the expression of the different molecular species of VGSCs because the neurons within each size class we examined belonged to different subclasses. Now that we have established the feasibility of pharmacologically fractionating the I_{Na} of DRG neurons, further work with DRG neurons belonging to more stringently defined subclasses is called for. For example, restricting the analyses to DRG neurons associated with either specific cell markers (Snape *et al.*, 2010), identified peripheral targets (Light *et al.*, 2008), specific sensory modalities (Teichert *et al.*, 2012), or a combination of these restrictions.

Variability in the levels of functional expression of the various Na_V1-isoforms was also apparent with SCG neurons (Figure 5 and Supporting Information Table S2). This variability may reflect experimental error, insofar as μ-TIIIA and μ-PIIIA were used at a concentration near their IC_{50}s for $Na_V1.3$; that is, near the steep part of their dose-response curves.

The observed results with DRG neurons in relation to other studies

In general, our results agree well with those of other types of studies. Adult DRG express messages for $Na_V1.1$, 1.6, 1.7, 1.8 and 1.9 (Rush *et al.*, 2007), and the major transcripts (in 1-week old rats) of small DRG neurons were $Na_V1.7$, 1.8 and 1.9, whereas those for large neurons were $Na_V1.1$, 1.6 and 1.7 (Ho and O'Leary, 2011). Expression of $Na_V1.2$ transcripts by DRG neurons has been reported (Black *et al.*, 1996; Ho and O'Leary, 2011); however, the functional expression of $Na_V1.2$ in the small and large neurons we examined appeared to be ruled out as mentioned above.

Immunohistochemistry has revealed that $Na_V1.6$ is present at nodes of Ranvier of all the peripheral myelinated axons, both motor and sensory, examined (Caldwell *et al.*, 2000). This is consistent with our previous results regarding the μ-conotoxin susceptibility of A-CAPs in rat sciatic nerve (Wilson *et al.*, 2011) as well as our present results that $Na_V1.6$ is associated with I_{Na} of large DRG neurons, insofar as large somas have axons with fast conduction velocities indicative of myelinated fibres (Harper and Lawson, 1985). Of interest in this regard is the observation that the I_{Na} of most of the 26 large neurons tested with μ-TIIIA were susceptible to the peptide, including two neurons where the major fraction (70%) of the I_{Na} was blocked by μ-TIIIA (Figure 4B), indicating that $Na_V1.1$ can be the dominant channel is some large cells. As shown in Table 3, all nine large neurons examined had significant levels (≈20%) of functional expression of $Na_V1.1$. This raises the question of whether and where might $Na_V1.1$ be in axons of large neurons.

Results from an immunohistochemical study demonstrated that both $Na_V1.1$ and $Na_V1.6$ are present at nodes of Ranvier of mouse CNS axons; in contrast, $Na_V1.6$, but not $Na_V1.1$, was observed in nodes of axons of dorsal and ventral roots (Duflocq *et al.*, 2008). This study also showed that motoneurons express $Na_V1.1$ non-uniformly in their initial axon segments, with a higher density located proximally than distally, and the converse pattern of expression was observed for $Na_V1.6$. The initial segment of DRG neurons is not where action potentials are (normally) initiated (see Amir and Devor, 2003), so similar variations in $Na_V1.1$ and 1.6 densities as that of motoneurons might not necessarily be expected. $Na_V1.1$ immunolabelling (unlike that of $Na_V1.6$, 1.7, 1.8 and 1.9) was absent at peripheral free nerve endings in adult rat skin (Persson *et al.*, 2010). Whether $Na_V1.1$ is located at central axon terminals of DRG neurons remains, as far as we are aware, to be determined.

Table 3 and Figure 6 suggest that $Na_V1.7$ can be functionally expressed by all DRG neurons, both large and small. Our previous results with C-CAPs of rat sciatic nerve indicated that $Na_V1.7$ was the major isoform responsible for propagation of action potentials in unmyelinated axons, but the methods used were too coarse to determine its possible contribution to A-CAPs, which are mediated by myelinated axons (Wilson *et al.*, 2011).

Our results provide a strong incentive to examine the specific roles and locations of the non-dominant Na_V1-isoforms in the processes of both small and large DRG neurons. It would be interesting in future studies to quantify the functional contributions of specific Na_V1-isoforms in intermediate-sized DRG neurons as well. Recent efforts in various laboratories to identify the molecular determinants for Na_V1-isoform specificity as well as obtain μ-conotoxins with improved selectivity have produced encouraging results (Leipold *et al.*, 2011; McArthur *et al.*, 2011; Van Der Haegen *et al.*, 2011) and bode well for future work in pharmacologically fractionating sodium currents with μ-conotoxins.

Conclusion

μ-Conotoxins provide evidence for the functional expression of three TTX-sensitive Na_V1-isoforms in both small and large DRG neurons as well as in SCG neurons. To our knowledge, this is the first attempt to quantitatively assess the relative contributions of specific Na_V1-isoforms to the TTX-sensitive I_{Na} of individual neurons in any preparation.

Acknowledgements

We thank Dr. Jozsef Gulyas and William Low for peptide synthesis and characterization.

This work was supported by the National Institutes of Health grant GM 48677 to G.B., B.M.O., J.E.R. and D.Y.

Conflict of interest

B.M.O. is a co-founder of Cognetix, Inc. and G.B. is a co-founder of NeuroAdjuvants, Inc.

References

Amir R, Devor M (2003). Electrical excitability of the soma of sensory neurons is required for spike invasion of the soma, but not for through-conduction. Biophys J 84: 2181–2191.

Black JA, Dib-Hajj S, McNabola K, Jeste S, Rizzo MA, Kocsis JD *et al.* (1996). Spinal sensory neurons express multiple sodium channel alpha-subunit mRNAs. Brain Res Mol Brain Res 43: 117–131.

Black JA, Liu S, Tanaka M, Cummins TR, Waxman SG (2004). Changes in the expression of tetrodotoxin-sensitive sodium channels within dorsal root ganglia neurons in inflammatory pain. Pain 108: 237–247.

Blair NT, Bean BP (2002). Roles of tetrodotoxin (TTX)-sensitive Na+ current, TTX-resistant Na+ current, and Ca2+ current in the action potentials of nociceptive sensory neurons. J Neurosci 22: 10277–10290.

Brackenbury WJ, Isom LL (2011). Na channel β subunits: overachievers of the ion channel family. Front Pharmacol 2: 53.

Brock JA, McLachlan E, Belmonte C (1998). Tetrodotoxin-resistant impulses in single nociceptor nerve terminals in guinea-pig cornea. J Physiol (Lond) 512 (Pt 1): 211–217.

Caffrey JM, Eng DL, Black JA, Waxman SG, Kocsis JD (1992). Three types of sodium channels in adult rat dorsal root ganglion neurons. Brain Res 592: 283–297.

Caldwell JH, Schaller KL, Lasher RS, Peles E, Levinson SR (2000). Sodium channel Na(v)1.6 is localized at nodes of ranvier, dendrites, and synapses. Proc Natl Acad Sci U S A 97: 5616–5620.

Catterall WA (2010). Ion channel voltage sensors: structure, function, and pathophysiology. Neuron 67: 915–928.

Catterall WA, Goldin AL, Waxman SG (2005). International Union of Pharmacology. XLVII. Nomenclature and structure-function relationships of voltage-gated sodium channels. Pharmacol Rev 57: 397–409.

Catterall WA, Cestele S, Yarov-Yarovoy V, Yu FH, Konoki K, Scheuer T (2007). Voltage-gated ion channels and gating modifier toxins. Toxicon 49: 124–141.

Chahine M, O'Leary ME (2011). Regulatory role of voltage-gated Na channel β subunits in sensory neurons. Front Pharmacol 2: 70.

Choi JS, Hudmon A, Waxman SG, Dib-Hajj SD (2006). Calmodulin regulates current density and frequency-dependent inhibition of sodium channel Nav1.8 in DRG neurons. J Neurophysiol 96: 97–108.

Dib-Hajj SD, Waxman SG (2010). Isoform-specific and pan-channel partners regulate trafficking and plasma membrane stability; and alter sodium channel gating properties. Neurosci Lett 486: 84–91.

Dib-Hajj SD, Fjell J, Cummins TR, Zheng Z, Fried K, LaMotte R *et al.* (1999). Plasticity of sodium channel expression in DRG neurons in the chronic constriction injury model of neuropathic pain. Pain 83: 591–600.

Dib-Hajj SD, Cummins TR, Black JA, Waxman SG (2010). Sodium channels in normal and pathological pain. Annu Rev Neurosci 33: 325–347.

Duflocq A, Le Bras B, Bullier E, Couraud F, Davenne M (2008). Nav1.1 is predominantly expressed in nodes of Ranvier and axon initial segments. Mol Cell Neurosci 39: 180–192.

Elliott AA, Elliott JR (1993). Characterization of TTX-sensitive and TTX-resistant sodium currents in small cells from adult rat dorsal root ganglia. J Physiol (Lond) 463: 39–56.

Fiedler B, Zhang MM, Buczek O, Azam L, Bulaj G, Norton RS *et al.* (2008). Specificity, affinity and efficacy of iota-conotoxin RXIA, an agonist of voltage-gated sodium channels Na(V)1.2, 1.6 and 1.7. Biochem Pharmacol 75: 2334–2344.

Fukuoka T, Kobayashi K, Yamanaka H, Obata K, Dai Y, Noguchi K (2008). Comparative study of the distribution of the alpha-subunits of voltage-gated sodium channels in normal and axotomized rat dorsal root ganglion neurons. J Comp Neurol 510: 188–206.

Goldin AL, Barchi RL, Caldwell JH, Hofmann F, Howe JR, Hunter JC *et al.* (2000). Nomenclature of voltage-gated sodium channels. Neuron 28: 365–368.

Harper AA, Lawson SN (1985). Conduction velocity is related to morphological cell type in rat dorsal root ganglion neurones. J Physiol 359: 31–46.

Herzog RI, Cummins TR, Ghassemi F, Dib-Hajj SD, Waxman SG (2003). Distinct repriming and closed-state inactivation kinetics of Nav1.6 and Nav1.7 sodium channels in mouse spinal sensory neurons. J Physiol (Lond) 551 (Pt 3): 741–750.

Hille B (2001). Ion Channels of Excitable Membranes, 3rd edn. Sinauer Associates: Sunderland, MA.

Ho C, O'Leary ME (2011). Single-cell analysis of sodium channel expression in dorsal root ganglion neurons. Mol Cell Neurosci 46: 159–166.

Kilkenny C, Browne W, Cuthill IC, Emerson M, Altman DG (2010). NC3Rs Reporting Guidelines Working Group. Br J Pharmacol 160: 1577–1579.

Leipold E, Markgraf R, Miloslavina A, Kijas M, Schirmeyer J, Imhof D *et al.* (2011). Molecular determinants for the subtype specificity of μ-conotoxin SIIIA targeting neuronal voltage-gated sodium channels. Neuropharmacology 61: 105–111.

Lewis RJ, Schroeder CI, Ekberg J, Nielsen KJ, Loughnan M, Thomas L *et al.* (2007). Isolation and structure-activity of mu-conotoxin TIIIA, a potent inhibitor of tetrodotoxin-sensitive voltage-gated sodium channels. Mol Pharmacol 71: 676–685.

Lewis RJ, Dutertre S, Vetter I, Christie MJ (2012). Conus venom peptide pharmacology. Pharmacol Rev 64: 259–298.

Light AR, Hughen RW, Zhang J, Rainier J, Liu Z, Lee J (2008). Dorsal root ganglion neurons innervating skeletal muscle respond to physiological combinations of protons, ATP, and lactate mediated by ASIC, P2X, and TRPV1. J Neurophysiol 100: 1184–1201.

Liu P, Jo S, Bean BP (2012). Modulation of neuronal sodium channels by the sea anemone peptide BDS-I. J Neurophysiol 107: 3155–3167.

McArthur JR, Singh G, McMaster D, Winkfein R, Tieleman DP, French RJ (2011). Interactions of key charged residues contributing to selective block of neuronal sodium channels by μ-conotoxin KIIIA. Mol Pharmacol 80: 573–584.

McGrath J, Drummond G, McLachlan E, Kilkenny C, Wainwright C (2010). Guidelines for reporting experiments involving animals: the ARRIVE guidelines. Br J Pharmacol 160: 1573–1576.

Momin A, Wood JN (2008). Sensory neuron voltage-gated sodium channels as analgesic drug targets. Curr Opin Neurobiol 18: 383–388.

Ogata N, Tatebayashi H (1992). Ontogenic development of the TTX-sensitive and TTX-insensitive Na+ channels in neurons of the rat dorsal root ganglia. Brain Res Dev Brain Res 65: 93–100.

Persson A-K, Black JA, Gasser A, Cheng X, Fischer TZ, Waxman SG (2010). Sodium-calcium exchanger and multiple sodium channel isoforms in intra-epidermal nerve terminals. Mol Pain 6: 84.

Roy ML, Narahashi T (1992). Differential properties of tetrodotoxin-sensitive and tetrodotoxin-resistant sodium channels in rat dorsal root ganglion neurons. J Neurosci 12: 2104–2111.

Rush AM, Dib-Hajj SD, Liu S, Cummins TR, Black JA, Waxman SG (2006). A single sodium channel mutation produces hyper- or hypoexcitability in different types of neurons. Proc Natl Acad Sci U S A 103: 8245–8250.

Rush AM, Cummins TR, Waxman SG (2007). Multiple sodium channels and their roles in electrogenesis within dorsal root ganglion neurons. J Physiol 579 (Pt 1): 1–14.

Shon KJ, Olivera BM, Watkins M, Jacobsen RB, Gray WR, Floresca CZ *et al.* (1998). mu-Conotoxin PIIIA, a new peptide for discriminating among tetrodotoxin-sensitive Na channel subtypes. J Neurosci 18: 4473–4481.

Snape A, Pittaway JF, Baker MD (2010). Excitability parameters and sensitivity to anemone toxin ATX-II in rat small diameter primary sensory neurones discriminated by Griffonia simplicifolia isolectin IB4. J Physiol 588 (Pt 1): 125–137.

Strassman AM, Raymond SA (1999). Electrophysiological evidence for tetrodotoxin-resistant sodium channels in slowly conducting dural sensory fibers. J Neurophysiol 81: 413–424.

Teichert RW, Raghuraman S, Memon T, Cox JL, Foulkes T, Rivier JE *et al*. (2012). Characterization of two neuronal subclasses through constellation pharmacology. Proc Natl Acad Sci U S A 109: 12758–12763.

Terlau H, Olivera BM (2004). Conus venoms: a rich source of novel ion channel-targeted peptides. Physiol Rev 84: 41–68.

Van Der Haegen A, Peigneur S, Tytgat J (2011). Importance of position 8 in mu-conotoxin KIIIA for voltage-gated sodium channel selectivity. FEBS J 278: 3408–3418.

Villière V, McLachlan EM (1996). Electrophysiological properties of neurons in intact rat dorsal root ganglia classified by conduction velocity and action potential duration. J Neurophysiol 76: 1924–1941.

Waxman SG, Kocsis JD, Black JA (1994). Type III sodium channel mRNA is expressed in embryonic but not adult spinal sensory neurons, and is reexpressed following axotomy. J Neurophysiol 72: 466–470.

West PJ, Bulaj G, Garrett JE, Olivera BM, Yoshikami D (2002). Mu-conotoxin SmIIIA, a potent inhibitor of tetrodotoxin-resistant sodium channels in amphibian sympathetic and sensory neurons. Biochemistry 41: 15388–15393.

Wilson MJ, Yoshikami D, Azam L, Gajewiak J, Olivera BM, Bulaj G *et al*. (2011). μ-Conotoxins that differentially block sodium channels NaV1.1 through 1.8 identify those responsible for action potentials in sciatic nerve. Proc Natl Acad Sci U S A 108: 10302–10307.

Zhang MM, Fiedler B, Green BR, Catlin P, Watkins M, Garrett JE *et al*. (2006). Structural and functional diversities among mu-conotoxins targeting TTX-resistant sodium channels. Biochemistry 45: 3723–3732.

Zhang MM, Green BR, Catlin P, Fiedler B, Azam L, Chadwick A *et al*. (2007). Structure/function characterization of micro-conotoxin KIIIA, an analgesic, nearly irreversible blocker of mammalian neuronal sodium channels. J Biol Chem 282: 30699–30706.

Zhang MM, McArthur JR, Azam L, Bulaj G, Olivera BM, French RJ *et al*. (2009). Synergistic and antagonistic interactions between tetrodotoxin and mu-conotoxin in blocking voltage-gated sodium channels. Channels (Austin) 3: 32–38.

Zhang MM, Gruszczynski P, Walewska A, Bulaj G, Olivera BM, Yoshikami D (2010). Cooccupancy of the outer vestibule of voltage-gated sodium channels by micro-conotoxin KIIIA and saxitoxin or tetrodotoxin. J Neurophysiol 104: 88–97.

Zhang MM, Wilson MJ, Azam L, Gajewiak J, Rivier JE, Bulaj G *et al*. (2012). Co-expression of $Na_V\beta$ subunits alters the kinetics of inhibition of voltage-gated sodium channels by pore-blocking μ-conotoxins. Br J Pharmacol 168: 1597–1610.

Supporting information

Additional Supporting Information may be found in the online version of this article at the publisher's web-site:

Figure S1 Time course of block of I_{Na} of SCG neurons by μ-TIIIA, μ-PIIIA or μ-SmIIIA, each tested individually at a concentration of 10 μM. Recordings of I_{Na} were acquired as described in Methods. These experiments parallel those illustrated in Figure 2 for DRG neurons. Plotted are peaks of I_{Na} obtained every 20 s before, during, and after exposure to indicated μ-conotoxin, denoted by bar at top of each plot. Each plot is an example from a different cell. Nearly complete block of I_{Na} was achieved by μ-SmIIIA, whose reversibility was much slower than those of the other two μ-conotoxins. Data are from neurons 1203c, 1204d and 2104b in Supporting Information Table S2.

Table S1 Properties of 32 small neurons (left eight columns) and 41 large neurons (right eight columns), including their toxin sensitivities. All DRG neurons used in this study are represented.

Table S2 Properties of 21 SCG neurons tested for their μ-conotoxin sensitivities. All SCG neurons used in this study are represented.

Table S3 Predicted contributions of Na_V1-isoforms to I_{Na} of SCG neurons[a].